Journal of Reproduction and Development, Vol. 68, No 3, 2022

Original Article

Expression and localization of tight junction-related proteins in adult rat pituitary stem/progenitor cell niches

Saishu YOSHIDA[1–4], Hideaki YURINO[5], Masaaki KOBAYASHI[1–3], Naoto NISHIMURA[1, 3], Kentaro YANO[1–3], Ken FUJIWARA[6], Shin-ichi HASHIMOTO[5], Takako KATO[2, 3] and Yukio KATO[1–3]

[1)]*Division of Life Science, Graduate School of Agriculture, Meiji University, Kanagawa 214-8571, Japan*
[2)]*Organization for the Strategic Coordination of Research and Intellectual Property, Meiji University, Kanagawa 214-8571, Japan*
[3)]*Institute of Endocrinology, Meiji University, Kanagawa 214-8571, Japan*
[4)]*Department of Biochemistry, The Jikei University School of Medicine, Tokyo 105-8461, Japan*
[5)]*Graduate School of Medical Sciences, Kanazawa University, Kanazawa 920-0934, Japan*
[6)]*Department of Biological Science, Kanagawa University, Kanagawa 259-1293 Japan*

Abstract. Pituitary endocrine cells are supplied by *Sox2*-expressing stem/progenitor cells in the anterior lobe of the adult pituitary gland. These SOX2-positive cells are maintained in two types of microenvironments (niches): the marginal cell layer (MCL)-niche and the parenchymal-niche. Recently, we isolated dense SOX2-positive cell clusters from the parenchymal-niche by taking advantage of their resistance to protease treatment as parenchymal stem/progenitor cell (PS)-clusters. In the present study, by analyzing these isolated PS-clusters, we attempted to identify novel structural characteristics of pituitary stem/progenitor cell niches. Quantitative real-time PCR showed that tight junction-related genes were distinctly expressed in the isolated PS-clusters. Immunocytostaining showed that the tight junction molecules, ZO-1 and occludin, were localized in the apical membrane facing the pseudo-follicle-like structure of the isolated PS-clusters regardless of the expression of *S100β*, which distinguishes the sub-population of SOX2-positive cells. Furthermore, immunohistochemistry of the pituitary glands of adult rats clearly demonstrated that ZO-1 and occludin were densely present in the parenchymal-niche encircling the pseudo-follicle, while they were observed in the apical membrane in the MCL-niche facing the residual lumen. Collectively, these tight junction-related proteins might be involved in the architecture and maintenance of the plasticity of pituitary stem/progenitor cell niches.

Key words: Rat pituitary, Stem cell niche, Stem/progenitor cells, Tight junction

(**J. Reprod. Dev. 68:** 225–231, 2022)

The pituitary gland is an important endocrine tissue composed of three lobes: the anterior, intermediate, and posterior lobes. The anterior lobe has five endocrine cell types that produce six hormones, and other non-endocrine cells. Some of the non-endocrine cells play roles in the support and supply of endocrine cells [1, 2]. Recent studies have demonstrated that cells expressing the sex-determining region Y-box 2 (*Sox2*) play important roles as stem/progenitor cells in the adult pituitary gland *in vitro* [3] and *in vivo* [4]. *S100β*-expressing cells, which are typical non-endocrine cells that perform multiple functions in the anterior lobe [5], may harbor stem/progenitor cell characteristics [6].

Several studies have demonstrated that SOX2-positive cells form two types of niches (stem/progenitor cell microenvironments): the marginal cell layer (MCL)-niche facing the residual lumen of Rathke's pouch and the parenchymal-niche composed of SOX2-positive cells scattered in the parenchyma of the adult anterior lobe [2, 7, 8]. Chen *et al*. showed that epithelial-mesenchymal transition (EMT) is preceded by alteration of apical membrane localization of the coxsackievirus and adenovirus receptor (CAR, a protein closely associated with tight junctions) to the basolateral membrane, followed by migration to the parenchyma and the formation of dense SOX2-positive clusters that encircle the pseudo-follicle [6, 7]. The dense SOX2-positive stem/progenitor cell clusters termed as "parenchymal stem/progenitor cell (PS)-clusters" have previously been isolated by taking advantage of their resistance to protease treatment [9]. Moreover, using the anterior lobe of S100β/green fluorescent protein-transgenic (S100β/GFP-TG) rats, PS-clusters have been classified into GFP-, mixed-GFP-, and null-GFP-clusters based on S100β-GFP signals exhibiting different proliferation and differentiation properties [9, 10]. Hence, PS-clusters provide a clue to elucidate the regulatory mechanism of pituitary stem/progenitor cell niches.

Notably, specific topographic affinities for adherens junctions, gap junctions, and tight junctions between pituitary endocrine and non-endocrine cells are known [11, 12]. E-cadherin is expressed in the pituitary adherens junction in S100β-positive and SOX2-positive cells [3, 13, 14], while gap junctions are present in most S100β-positive cells and are assumed to play important roles in the anterior lobe [15, 16]. The tight junction, a topical structure of epithelial and endothelial cells, is important for cell-to-cell adhesion, acts as a barrier for cell migration, and separation of apical and basolateral fluid compartments by polar localization [17]. Two types of tight junction-related proteins are known namely, integral transmembrane

Received: December 18, 2021
Accepted: March 18, 2022
Advanced Epub: April 12, 2022

Correspondence: S Yoshida (e-mail: saishu@jikei.ac.jp)

proteins [18] and tight junctional plaque proteins [19]. The former type forms homo- and heterophilic interactions with occludin (a member of claudin), junction adhesion molecules (JAMs), and other cortical thymocyte markers in the *Xenopus* (CTX) subfamily [18]. The latter type may link the cytoplasmic domains of transmembrane proteins with the actin cytoskeleton or cellular signaling molecules, including zonula occludens (ZO)-1, ZO-2, ZO-3, cingulin, and α-catenin. In the anterior lobe, the expression of claudin-4 and claudin-2 and -5 are observed in S100β-positive cells and endothelial cells, respectively [20]. More recently, Higashi *et al*. reported that claudin-9 is specifically expressed in S100β-positive cells [21]. However, whether tight junction-related proteins exist in the pituitary stem/progenitor cell niches remains unclear.

In the present study, we attempted to identify a novel characteristic structure of pituitary stem/progenitor cell niches using gene expression analysis and immunostaining of isolated PS-clusters. Collectively, we demonstrated that tight junction-related proteins were present and might be involved in the architecture and maintenance of plasticity of pituitary stem/progenitor cell niches.

Materials and Methods

Animals

Wistar-crlj S100β/green fluorescent protein-transgenic rats (S100β/GFP-TG rats), that were generated by fusing the *S100*β promoter to the reporter gene *Gfp* [22] (male, 8–16 weeks), were housed individually in a temperature-controlled room under a 12-h light/12-h dark cycle. The rats were euthanized under anesthesia. This study was approved by the Institutional Animal Care and Use Committee of Meiji University and complied with the NIH Guidelines for the Care and Use of Laboratory Animals.

Pituitary cell dispersion and isolation of PS-clusters

Cell dispersion of the anterior lobe of the rat pituitary and isolation of PS-clusters were performed according to a previous report [9]. Briefly, excised anterior lobes of the pituitaries from S100β/GFP-TG rats were treated with 0.2% collagenase (Sigma-Aldrich, St. Louis, MO, USA) for 15 min at 37°C. After removal of the collagenase solution, collected cells were incubated with 10 mM HEPES-100 mM NaCl (pH 7.5; HEPES buffer) containing 0.25% trypsin (Sigma-Aldrich), and 5 mM EDTA (Dojindo Laboratories, Kumamoto, Japan) for 10 min at 37°C and dispersed by vigorous pipetting. The cell suspension was plated on a non-adhesive 35-mm dish (AGC Techno Glass, Shizuoka, Japan), and PS-clusters were immediately collected manually using pipettes, under a microscope (Leica DM IRB, Leica, Wetzlar, Germany).

cDNA library preparation and quantitative real-time polymerase chain reaction (PCR)

cDNA libraries were prepared according to a previously reported method [10] with slight modifications. Briefly, cDNA was synthesized from isolated GFP-clusters, null-GFP-clusters, and whole cells of the anterior lobe, and three independent experiments were performed [23] using SuperScript II Reverse Transcriptase (Thermo Fisher Scientific, Waltham, MA, USA) and KAPA HiFi HotStart ReadyMix (NIPPON Genetics, Tokyo, Japan). The synthesized cDNA was purified using AMPure XP (Beckman Coulter, Brea, CA, USA). Quantitative real-time PCR was performed using SYBR Green Real-Time PCR Master Mix Plus (Toyobo, Osaka, Japan) and 0.6 μM of specific primer set for nine genes (Table 1), and analyzed using the Applied Biosystems StepOnePlus Real-Time PCR system (Applied Biosystems, Foster City, CA, USA). *Hprt1* (hypoxanthine phosphoribosyltransferase 1) was used as an internal standard and fold change was calculated by comparing the expression levels relative to those of whole cells. Data are presented as the mean ± SEM (n = 3). The DNA sequence of the PCR product from each sample was confirmed by nucleotide sequencing (data not shown). One-way analysis of variance (ANOVA) followed by Tukey's test for

Table 1. List of primer sets for quantitative real-time PCR

Protein name	Gene symbol Gene name		Sequence (5'→3')	Product size (bp)	Accession number
ZO-1	*Tjp1* *Tight junction protein 1*	Forward Reverse	ctgagccccctagtgatgtg acagaaacacagttggctccaac	149	NM_001106266.1
ZO-2	*Tjp2* *Tight junction protein 2*	Forward Reverse	atgcggttccaatcaaagc ctcttcctcgggatcactgc	134	NM_053773.1
ZO-3	*Tjp3* *Tight junction protein 3*	Forward Reverse	gatgggtcatgggaggatcg ttctcagggcctcatgcttg	110	NM_001108073.1
Cingulin	*Cgn* *Cingulin*	Forward Reverse	tccaagcccggatcaaatcc atgcaatggatgaggggtcg	138	XM_017591315.1
Occludin	*Ocln* *Occludin*	Forward Reverse	caacggcaaagtgaatggcaag atcgttgctgctgtaccgag	139	NM_031329.2
JAM1	*Jam1* (*F11r*) *Junctional adhesion molecule 1*	Forward Reverse	gaccctgtgtcagcctttga agtgttaccaggacagctgc	143	NM_053796.1
JAM2	*Jam2* *Junctional adhesion molecule 2*	Forward Reverse	aactctgttgggcatcgcag gcagaaatgacgaaggccac	107	NM_001034004.1
JAM3	*Jam3* *Junctional adhesion molecule 3*	Forward Reverse	tcacaatgggcatctgctgtg caccctcttcacttgtccgg	126	NM_001004269.1
CAR	*Cxadr* *Coxsackievirus and adenovirus receptor*	Forward Reverse	aaccaagtccccagtgaaga aatgccatcggtcaggtaag	93	NM_053570.1
HPRT1	*Hprt1* *Hypoxanthine phosphoribosyltransferase 1*	Forward Reverse	ctcatggactgattatggacaggac gcaggtcagcaaagaacttatagcc	123	NM_012583.2

multiple comparisons was performed using Prism Ver. 7 (GraphPad Software, San Diego, CA, USA).

Immunocytostaining of isolated PS-clusters

To attach PS-clusters onto eight-well chamber slides (Thermo Fisher Scientific) and recover cell surface proteins, isolated PS-clusters were transferred into wells of Matrigel-coated glass slides using growth factor-reduced Matrigel diluted 1:10 with DMEM/F-12 serum-free medium (BD Biosciences, San Jose, CA, USA) and incubated for 4–7 h in a humidified atmosphere of 5% CO_2 and 95% air. After attachment, PS-clusters were fixed with 4% paraformaldehyde (PFA) in 20 mM HEPES (pH 7.5) for 30 min at 20–25°C. Samples were antigen-retrieved using ImmunoSaver (0.05% citraconic anhydride solution, pH 7.4; Nisshin EM, Tokyo, Japan) for 1 h at 80°C. Cells were incubated with 10% (v/v) fetal bovine serum and 0.4% (v/v) Triton X-100 in HEPES buffer (blocking buffer) for 60 min at room temperature. The primary antibody reaction was performed in blocking buffer overnight at 4°C using goat IgG against human SOX2 (GT15098; 1:500, Neuromics, Edina, MN, USA), rabbit IgG against human ZO-1 (SA243690; 1:20,000, Thermo Fisher Scientific), rabbit IgG against human occludin (RG235307; 1:2,000, Thermo Fisher Scientific), and chicken IgY against jellyfish GFP (GFP-1020; 1:500, Aves Labs, Tigard, OR, USA). After the immunoreaction, cells were incubated with secondary antibodies in blocking buffer for 2 h at 4°C using Cy3-, Cy5-, or FITC-conjugated AffiniPure donkey anti-goat, rabbit IgG, and chicken IgY (1:500; Jackson ImmunoResearch, West Grove, PA, USA). Cells were washed and incubated with VECTASHIELD mounting medium (Vector Laboratories, Burlingame, CA, USA) with 4′,6-diamidino-2-phenylindole dihydrochloride (DAPI). Immunofluorescence was observed using the DMI6000 B inverted microscope (Leica, Wetzlar, Germany).

Immunohistochemistry

The pituitaries of male S100β/GFP-TG rats were fixed with 4% PFA overnight at 4°C, followed by immersion in 30% trehalose in 20 mM HEPES to cryoprotect the tissues. They were embedded in Tissue-Tek O.C.T. compound (Sakura Finetek Japan, Tokyo, Japan) and frozen immediately. Frozen sections (6-µm thick) from the coronal planes of the pituitaries were prepared. The sections were antigen-retrieved using ImmunoSaver (Nisshin EM) for 1 h at 80°C. After washing, the sections were incubated with primary antibodies (as described above) in blocking buffer overnight at 4°C. After the immunoreaction, the sections were incubated with secondary antibodies (as described above). The sections were washed and then stained with DAPI (Vector Laboratories). Immunofluorescence was observed using the BZ-8000 fluorescence microscope (Keyence, Osaka, Japan).

Results

Gene expression of tight junction-related proteins in isolated PS-clusters

To identify novel structural characteristics of pituitary stem/progenitor cell niches, we examined gene expression in isolated PS-clusters (Fig. 1A and 1B) by qPCR. Based on our previous report that CAR (encoded by *Cxadr*) is expressed in pituitary stem/progenitor cell niches [7, 24], we focused on tight junction-related molecules. First, significant expression of CAR in both GFP- and null-GFP-clusters was confirmed (Fig. 1C). We then analyzed the expression of junctional plaque proteins such as, ZOs (ZO-1, ZO-2, and ZO-3 encoded by *Tjp1*, *Tjp2*, and *Tjp3*, respectively), and cingulin (encoded by *Cgn*; a scaffold protein). qPCR demonstrated

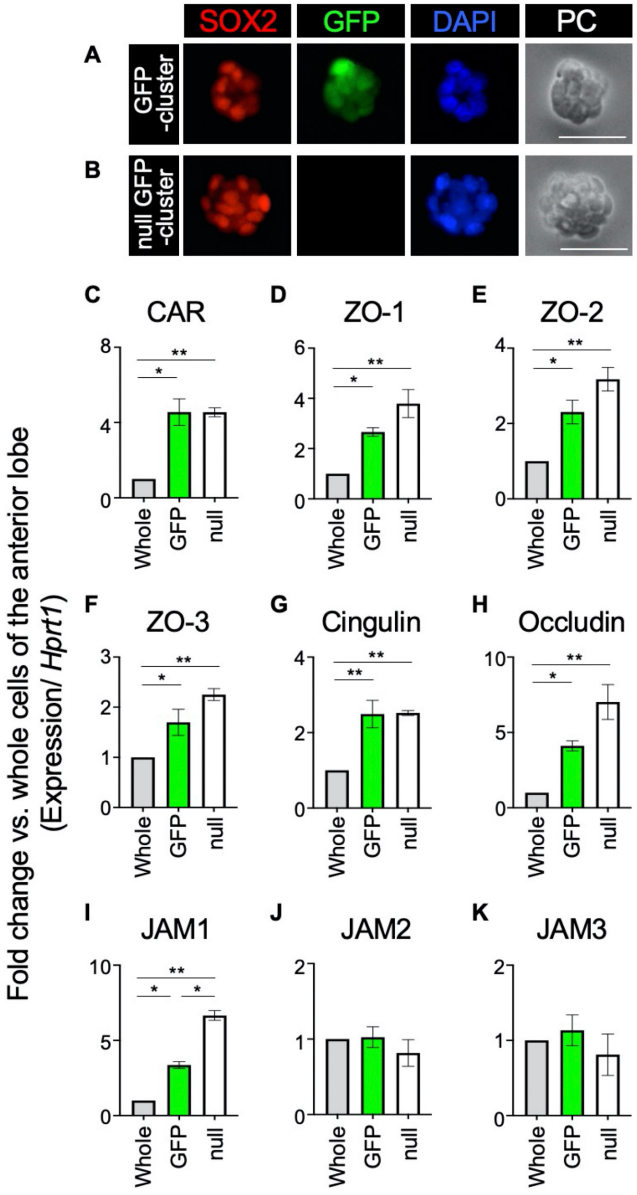

Fig. 1. Expression of tight junction-related genes in isolated GFP- and null-GFP-clusters from the anterior lobe of adult S100β/GFP-TG rats. Immunocytostaining was performed for SOX2 and GFP in the isolated GFP-cluster (A) and null-GFP-cluster (B). SOX2 visualized with Cy3 (red), GFP with FITC (green), nuclear staining using DAPI (blue), and phase-contrast (PC) are shown. Bars indicate 20 µm. Quantitative real-time polymerase chain reaction (PCR) was performed to estimate the mRNA levels of CAR (C), tight junction proteins, ZO-1 (D), ZO-2 (E), ZO-3 (F), cingulin (G), occludin (H), and junctional adhesion molecules (JAM1: I, JAM2: J, and JAM3: K), using total RNA isolated from whole cells of the anterior lobe (whole), isolated GFP-clusters (GFP), and null-GFP-clusters (null). Hypoxanthine phosphoribosyltransferase 1 (*Hprt1*) was used as an internal standard, and fold change was calculated by comparing the expression levels relative to those of whole cells. Data are presented as the mean ± SEM (n = 3 biological replicates per condition). Statistical significance was determined by one-way ANOVA followed by Tukey's test for multiple comparisons. * $P < 0.05$, ** $P < 0.01$.

that ZO-1, ZO-2, ZO-3, and cingulin were significantly expressed in both GFP- and null-GFP-clusters compared to whole cells (Fig. 1D–1G). Furthermore, genes encoding occludin (encoded by *Ocln*; a transmembrane protein) and JAM1 were significantly expressed in

both GFP- and null-GFP-clusters compared to whole cells, while no significant differences were observed in genes encoding JAM2 and JAM3 (Fig. 1H–1K). In addition, JAM1 was significantly expressed in GFP-clusters compared to null-GFP-clusters (Fig. 1I).

Immunocytostaining for ZO-1 and occludin in isolated PS-clusters

To confirm the results of gene expression profiling of the isolated PS-clusters, we performed triple immunocytostaining for the representative tight-junction molecules, ZO-1 or occludin, with SOX2 and GFP (for detection of S100β), using isolated PS-clusters. The results demonstrated that immuno-positive signals for ZO-1 (Fig. 2A, 2B) and occludin (Fig. 2C, 2D) were similarly detected in the apical and basolateral membranes of isolated PS-clusters. These ZO-1 immuno-positive signals were detected in all the examined PS-clusters including, GFP-clusters (100 clusters, Fig. 2A) and null-GFP-clusters (22 clusters, Fig. 2B). Similar results were obtained for occludin immunocytostaining in both GFP-clusters (104 clusters, Fig. 2C) and null-GFP-clusters (12 clusters, Fig. 2D).

Immunohistochemistry for ZO-1 and occludin in the anterior lobe of pituitary gland of adult rats

Next, we performed immunohistochemistry for ZO-1 and occludin in the pituitary gland of adult S100β/GFP-TG rat. Triple immunostaining for ZO-1 or occludin with SOX2 and GFP demonstrated intense immunopositive signals for ZO-1 (Fig. 3) and occludin (Fig. 4) in SOX2-positive cells in the parenchymal-niche (yellow arrow). These immuno-positive signals for ZO-1 or occludin in the parenchymal-niche were detected in both GFP/SOX2-double positive (Fig. 3D, 4D) and GFP-negative/SOX2-positive cells (Fig. 3E, 4E), corresponding to the results obtained from immunocytostaining of isolated PS-clusters (Fig. 2).

In relation to the MCL-niche, immunohistochemistry demonstrated that intense immuno-positive signals for ZO-1 (Fig. 3) and occludin (Fig. 4) were detected only in the apical membrane of SOX2-positive cells in both the anterior and intermediate lobes (Fig. 3, 4, white arrows).

In addition, immuno-positive signals for ZO-1 and occludin were also detected in some SOX2-positive cells (Figs. 3, 4, arrowheads). In contrast, weak immuno-positive signals for ZO-1 (Fig. 3, asterisks) and occludin (not shown in Fig. 4, but confirmed in other fields) were detected in the apical membrane of cells located in the perivascular space of the anterior lobe.

Discussion

Recent studies have proposed that SOX2-positive stem/progenitor cells of the adult anterior lobe form two types of niches, and demonstrated that dense SOX2-positive PS-clusters can be isolated from the parenchymal-niche by taking advantage of its tight structure and resistance to protease treatment [9]. In the present study, by analyzing isolated PS-clusters, we attempted to identify novel structural characteristics of the pituitary stem/progenitor cell niches.

E-cadherin is known to act as a cell-to-cell adherens junction molecule that anchors pituitary stem/progenitor cells, in contrast to N-cadherin, which is localized in endocrine cells [9, 13, 14]. The present study showed that adherens junctions via E-cadherin and tight junction-related proteins exist in both the pituitary niches. In the anterior lobe, using freeze-fracture electron microscopy, tight junctions have been observed mainly in non-endocrine cells [16].

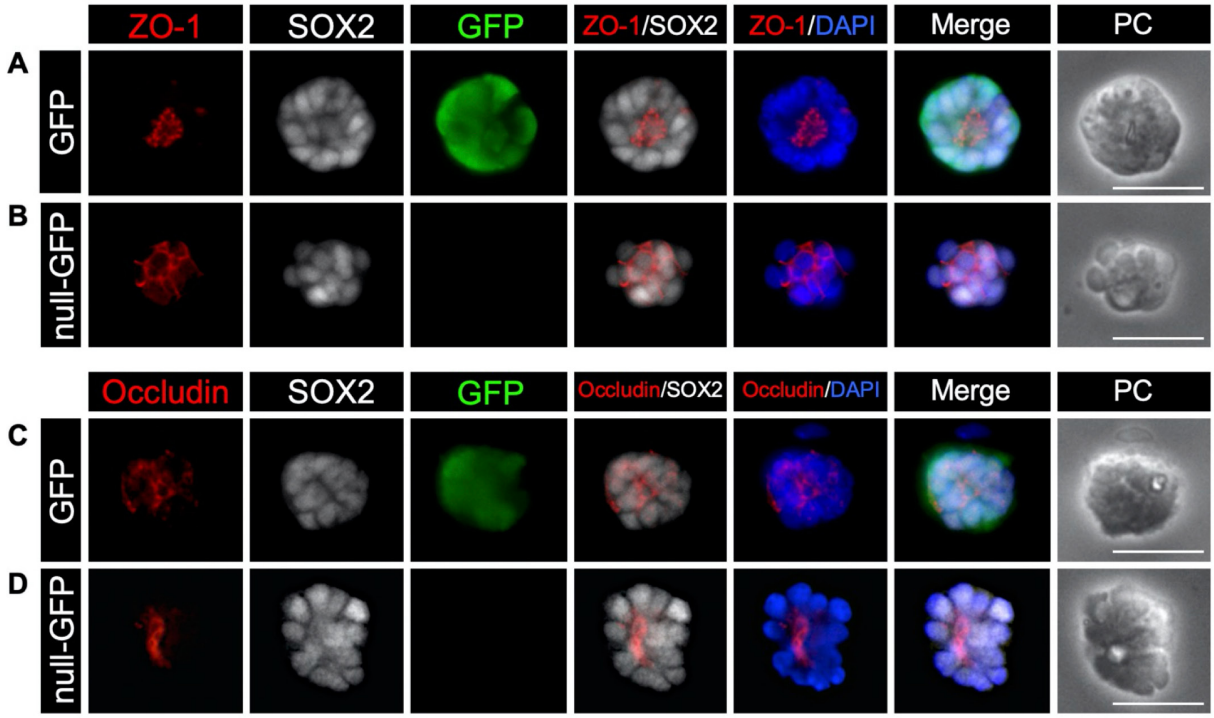

Fig. 2. Immunocytostaining for ZO-1 and occludin using isolated PS-clusters from the anterior lobe of adult S100β/GFP-TG rats. Immunocytostaining was performed for ZO-1 using isolated GFP-cluster (A) and null-GFP-cluster (B). ZO-1 visualized with Cy3 (red), SOX2 with Cy5 (white), GFP with FITC (green), merged images, and phase-contrast (PC) are shown. Immunocytostaining was performed for occludin using isolated GFP-cluster (C) and null-GFP-cluster (D). Occludin visualized with Cy3 (red), SOX2 with Cy5 (white), GFP with FITC (green), merged images, and phase-contrast (PC) are shown. Bars indicate 20 μm.

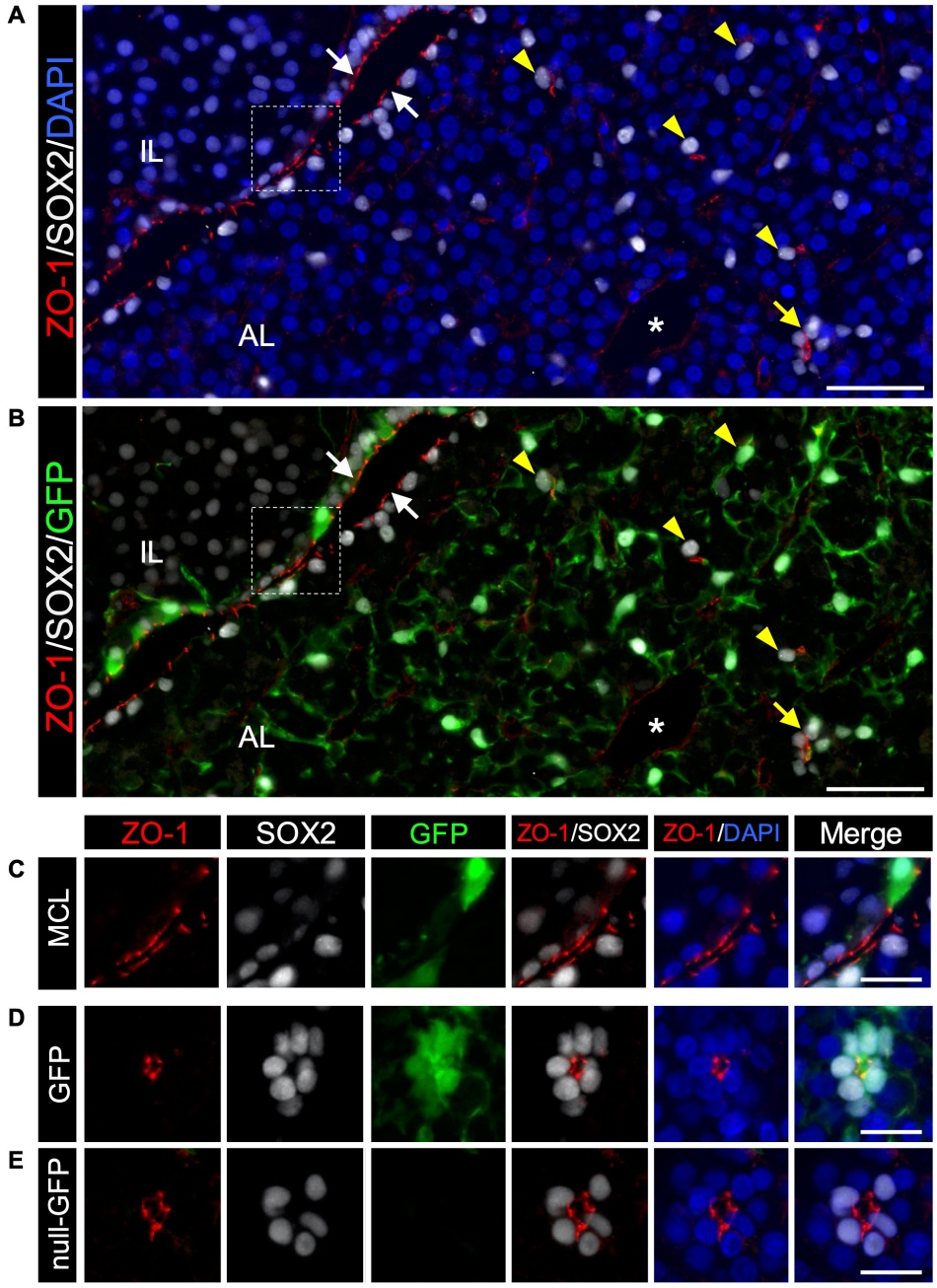

Fig. 3. Immunohistochemistry for ZO-1 using the anterior lobe of the pituitary. Immunohistochemistry for ZO-1, SOX2, and GFP was performed using 4% PFA-fixed frozen sections of the anterior lobe of adult S100β/GFP-TG rats. Merged images of ZO-1 visualized with Cy3 (red), SOX2 with Cy5 (white), and nuclear staining using DAPI (blue) (A) or GFP with FITC (green) (B), are shown. (B) Merged images of ZO-1 (red), SOX2 (white), and GFP with FITC (green) are shown. The areas in the boxes in (A) and (B) are enlarged in (C). Immunohistochemistry for ZO-1, SOX2, and GFP in S100β/GFP-positive (D) and S100β/GFP-negative (E) parenchymal-niches are shown. AL, anterior lobe; IL, intermediate lobe. White and yellow arrows indicate the MCL-niche and parenchymal-niche, respectively. Arrowheads indicate ZO-1-positive cells in SOX2-positive cells. * indicates the perivascular space of the anterior lobe. Bars indicate 50 μm (A, B) and 20 μm (C, D, and E).

In addition, some claudins are expressed in certain S100β-positive cells and endothelial cells [20]. Corresponding to these reports, we observed intense and weak immuno-positive signals for tight junction molecules in some S100β-positive cells and endothelial cells, respectively. Notably, our immunohistochemical analysis demonstrated that intense immuno-positive signals observed for the representative tight-junction molecules, ZO-1 and occludin, were also distinctly detected in SOX2-positive cells comprising the parenchymal- and MCL-niches. In the parenchymal-niche as well as isolated PS-clusters, immuno-positive signals for ZO-1 and occludin were observed in the apical and basolateral regions, whereas the signals in the MCL-niche were mainly observed on the apical surface facing the residual lumen (Figs. 3, 4). These distinct localizations of tight junction proteins between the MCL (apically facing residual lumen) and parenchymal (densely apicobasal-facing pseudo-follicle) niches may contribute to the difference in resistance to protease treatment. Moreover, our previous reports demonstrated that GFP- and null-GFP-clusters exhibit different proliferation and differentiation properties [9, 10]. Gene expression and immunochemical analyses revealed no distinct differences in the expression of tight junctions in this study. Further

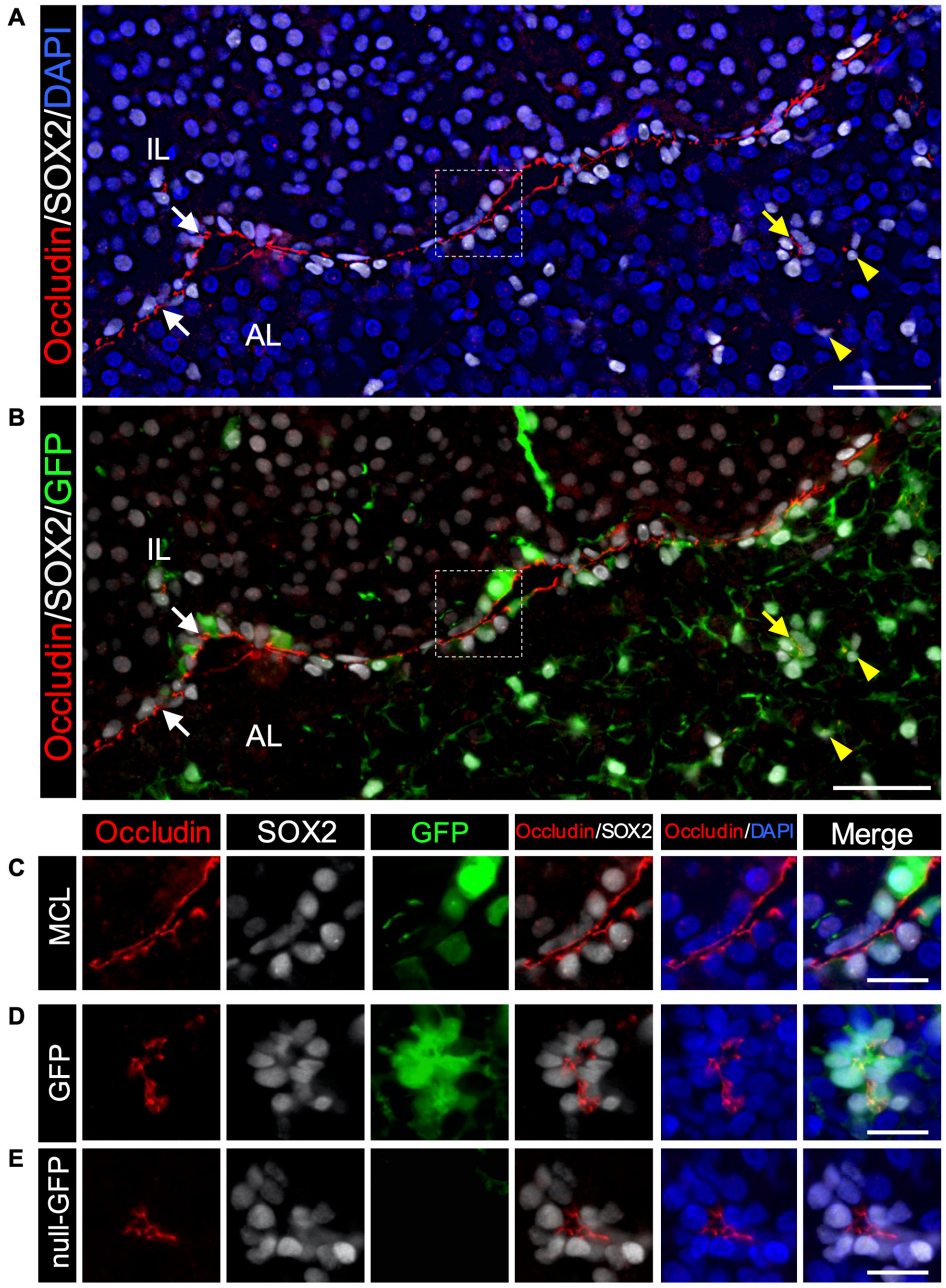

Fig. 4. Immunohistochemistry for occludin using the anterior lobe of the pituitary. Immunohistochemistry for occludin, SOX2, and GFP was performed using 4% PFA-fixed frozen sections of the anterior lobe of adult S100β/GFP-TG rats. Merged images of occludin visualized with Cy3 (red), SOX2 with Cy5 (white), and nuclear staining using DAPI (blue) (A) or GFP with FITC (green) (B), are shown. The areas in the boxes in (A) and (B) are enlarged in (C). Immunohistochemistry for occludin, SOX2, and GFP in S100β/GFP-positive (D) and S100β/GFP-negative (E) parenchymal-niches are shown. AL, anterior lobe; IL, intermediate lobe. White arrows and yellow arrows indicate the MCL-niche and parenchymal-niche, respectively. Arrowheads indicate occludin-positive cells in SOX2-positive cells. Bars indicate 50 μm (A, B) and 20 μm (C, D, and E).

investigation is required to elucidate the mechanism underlying the difference between GFP- and null-GFP-clusters.

The formation of rosette structures via tight junctions has been observed in the mouse neural stem cell niche [25, 26] and in human and mouse ES cells [27]. Martin *et al*. showed that tight junctions act as suppressors of cell migration [17]. Notably, knockdown of *ZO-1* in neural stem cells *in vitro* decreased the expression of neural stem cell markers, *Nestin* and *Sox2* [28], indicating that tight junction proteins are involved in the maintenance of stemness. Elucidation of the mechanism of EMT in the anterior lobe is also an intriguing issue, since the migration of pituitary stem/progenitor cells from the MCL-niche to the parenchyma is important for the maintenance of anterior lobe cell compartment. Previously, we demonstrated that CAR in the MCL-niche changes its localization from apical to basolateral during the process of EMT, and the stem/progenitor cells in the MCL-niche migrate to form the parenchymal-niche [7, 9]. The disassembly of epithelial cell-to-cell contacts (e.g., tight junctions, adherens junctions, desmosomes, and gap junctions) and cell polarization are the first steps in EMT. Notably, the EMT inducer SNAIL1, directly represses the expression of occludin [29] and *E-cadherin* [30]. Considering these reports, tight junction-related proteins in the pituitary stem/progenitor cell niches might be involved in the maintenance of stemness and

migration from their niches, accompanied by differentiation into endocrine cells. Further research is required to elucidate the role of tight junction-related proteins in pituitary stem/progenitor cell niches.

SOX2-positive cells are highly polarized, which is another characteristic feature of pituitary stem/progenitor cell niches. In addition to ZO-1 and occludin, immunohistochemical analysis showed that several molecules such as, CAR [7], ephrin-B2 [24], EphB3, and filamentous actin [31] showed polar localization in the apical membrane of both niches. Importantly, these molecules contain a PDZ (PSD-95, Dlg, ZO-1)-binding domain that interacts with multiple proteins containing PDZ domains, such as tight junction-associated proteins. Moreover, in the adult neural stem cell niche, apicobasal polarity of neural stem cells is important for their asymmetric division [32]. While asymmetric division of stem/progenitor cells has not been fully demonstrated in the pituitary, further studies regarding apicobasal polarity in the pituitary niches might reveal the significance of asymmetric division for migration and differentiation.

In summary, we demonstrated that tight junction-related proteins characteristically exist in two types of pituitary stem/progenitor cell niches. Further analysis of the molecular functions of the tight junctions in these niches might provide insights into the regulation of stemness, migration, and differentiation related to the supply and renewal of anterior pituitary cells.

Conflict of interests: The authors declare no conflicts of interest.

Acknowledgements

The authors, S.Y., Y.K., and T.K., wish to thank Dr. Y. Ito and Dr. S. Takekoshi (Division of Host Defense Mechanism, Tokai University) for their valuable suggestions regarding tight junction structures and molecules. The authors also wish to thank Mr. K. Kanno, Mr. Y. Tamura, Mr. R. Sekura, and Mr. T. Watanabe for their technical assistance. This work was partially supported by JSPS KAKENHI (grant numbers 21K06192, 16K18818, and 15J11564 to S.Y., 24580435 to T.K., and 26292166 to Y.K.), the MEXT-Supported Program for the Strategic Research Foundation at Private Universities, a research grant (A) to Y.K. from the Institute of Science and Technology, Meiji University, and Meiji University International Institute for BioResource Research (MUIIR), the Takeda Science Foundation (to S.Y.), and the Uehara Memorial Foundation (to S.Y.).

References

1. **Castinetti F, Davis SW, Brue T, Camper SA.** Pituitary stem cell update and potential implications for treating hypopituitarism. *Endocr Rev* 2011; **32**: 453–471. [Medline] [CrossRef]
2. **Vankelecom H, Chen J.** Pituitary stem cells: where do we stand? *Mol Cell Endocrinol* 2014; **385**: 2–17. [Medline] [CrossRef]
3. **Fauquier T, Rizzoti K, Dattani M, Lovell-Badge R, Robinson IC.** SOX2-expressing progenitor cells generate all of the major cell types in the adult mouse pituitary gland. *Proc Natl Acad Sci USA* 2008; **105**: 2907–2912. [Medline] [CrossRef]
4. **Andoniadou CL, Matsushima D, Mousavy Gharavy SN, Signore M, Mackintosh AI, Schaeffer M, Gaston-Massuet C, Mollard P, Jacques TS, Le Tissier P, Dattani MT, Pevny LH, Martinez-Barbera JP.** Sox2(+) stem/progenitor cells in the adult mouse pituitary support organ homeostasis and have tumor-inducing potential. *Cell Stem Cell* 2013; **13**: 433–445. [Medline] [CrossRef]
5. **Devnath S, Inoue K.** An insight to pituitary folliculo-stellate cells. *J Neuroendocrinol* 2008; **20**: 687–691. [Medline] [CrossRef]
6. **Kato Y, Yoshida S, Kato T.** New insights into the role and origin of pituitary S100β-positive cells. *Cell Tissue Res* 2021; **386**: 227–237. [Medline] [CrossRef]
7. **Chen M, Kato T, Higuchi M, Yoshida S, Yako H, Kanno N, Kato Y.** Coxsackievirus and adenovirus receptor-positive cells compose the putative stem/progenitor cell niches in the marginal cell layer and parenchyma of the rat anterior pituitary. *Cell Tissue Res* 2013; **354**: 823–836. [Medline] [CrossRef]
8. **Yoshida S, Kato T, Kato Y.** Regulatory system for stem/progenitor cell niches in the adult rodent pituitary. *Int J Mol Sci* 2016; **17**: 75. [Medline] [CrossRef]
9. **Yoshida S, Nishimura N, Ueharu H, Kanno N, Higuchi M, Horiguchi K, Kato T, Kato Y.** Isolation of adult pituitary stem/progenitor cell clusters located in the parenchyma of the rat anterior lobe. *Stem Cell Res (Amst)* 2016; **17**: 318–329. [Medline] [CrossRef]
10. **Yoshida S, Nishimura N, Yurino H, Kobayashi M, Horiguchi K, Yano K, Hashimoto SI, Kato T, Kato Y.** Differentiation capacities of PS-clusters, adult pituitary stem/progenitor cell clusters located in the parenchymal-niche, of the rat anterior lobe. *PLoS One* 2018; **13**: e0196029. [Medline] [CrossRef]
11. **Denef C.** Paracrinicity: the story of 30 years of cellular pituitary crosstalk. *J Neuroendocrinol* 2008; **20**: 1–70. [Medline]
12. **Tsukada T, Kouki T, Fujiwara K, Ramadhani D, Horiguchi K, Kikuchi M, Yashiro T.** Reassembly of anterior pituitary organization by hanging drop three-dimensional cell culture. *Acta Histochem Cytochem* 2013; **46**: 121–127. [Medline] [CrossRef]
13. **Chauvet N, El-Yandouzi T, Mathieu MN, Schlernitzauer A, Galibert E, Lafont C, Le Tissier P, Robinson IC, Mollard P, Coutry N.** Characterization of adherens junction protein expression and localization in pituitary cell networks. *J Endocrinol* 2009; **202**: 375–387. [Medline] [CrossRef]
14. **Kikuchi M, Yatabe M, Kouki T, Fujiwara K, Takigami S, Sakamoto A, Yashiro T.** Changes in E- and N-cadherin expression in developing rat adenohypophysis. *Anat Rec (Hoboken)* 2007; **290**: 486–490. [Medline] [CrossRef]
15. **Morand I, Fonlupt P, Guerrier A, Trouillas J, Calle A, Remy C, Rousset B, Munari-Silem Y.** Cell-to-cell communication in the anterior pituitary: evidence for gap junction-mediated exchanges between endocrine cells and folliculostellate cells. *Endocrinology* 1996; **137**: 3356–3367. [Medline] [CrossRef]
16. **Soji T, Herbert DC.** Intercellular communication between rat anterior pituitary cells. *Anat Rec* 1989; **224**: 523–533. [Medline] [CrossRef]
17. **Martin TA, Jiang WG.** Loss of tight junction barrier function and its role in cancer metastasis. *Biochim Biophys Acta* 2009; **1788**: 872–891. [Medline] [CrossRef]
18. **Barton ES, Forrest JC, Connolly JL, Chappell JD, Liu Y, Schnell FJ, Nusrat A, Parkos CA, Dermody TS.** Junction adhesion molecule is a receptor for reovirus. *Cell* 2001; **104**: 441–451. [Medline] [CrossRef]
19. **Zihni C, Mills C, Matter K, Balda MS.** Tight junctions: from simple barriers to multifunctional molecular gates. *Nat Rev Mol Cell Biol* 2016; **17**: 564–580. [Medline] [CrossRef]
20. **García-Godínez A, Contreras RG, González-Del-Pliego M, Aguirre-Benítez E, Acuña-Macías I, de la Vega MT, Martín-Tapia D, Solano-Agama C, Mendoza-Garrido ME.** Anterior and intermediate pituitary tissues express claudin 4 in follicle stellate cells and claudins 2 and 5 in endothelial cells. *Cell Tissue Res* 2014; **357**: 309–321. [Medline] [CrossRef]
21. **Higashi AY, Higashi T, Furuse K, Ozeki K, Furuse M, Chiba H.** Claudin-9 constitutes tight junctions of folliculo-stellate cells in the anterior pituitary gland. *Sci Rep* 2021; **11**: 21642. [Medline] [CrossRef]
22. **Itakura E, Odaira K, Yokoyama K, Osuna M, Hara T, Inoue K.** Generation of transgenic rats expressing green fluorescent protein in S-100beta-producing pituitary folliculo-stellate cells and brain astrocytes. *Endocrinology* 2007; **148**: 1518–1523. [Medline] [CrossRef]
23. **Picelli S, Faridani OR, Björklund AK, Winberg G, Sagasser S, Sandberg R.** Full-length RNA-seq from single cells using Smart-seq2. *Nat Protoc* 2014; **9**: 171–181. [Medline] [CrossRef]
24. **Yoshida S, Kato T, Higuchi M, Chen M, Ueharu H, Nishimura N, Kato Y.** Localization of juxtacrine factor ephrin-B2 in pituitary stem/progenitor cell niches throughout life. *Cell Tissue Res* 2015; **359**: 755–766. [Medline] [CrossRef]
25. **Harding MJ, McGraw HF, Nechiporuk A.** The roles and regulation of multicellular rosette structures during morphogenesis. *Development* 2014; **141**: 2549–2558. [Medline] [CrossRef]
26. **Mirzadeh Z, Merkle FT, Soriano-Navarro M, Garcia-Verdugo JM, Alvarez-Buylla A.** Neural stem cells confer unique pinwheel architecture to the ventricular surface in neurogenic regions of the adult brain. *Cell Stem Cell* 2008; **3**: 265–278. [Medline] [CrossRef]
27. **Elkabetz Y, Panagiotakos G, Al Shamy G, Socci ND, Tabar V, Studer L.** Human ES cell-derived neural rosettes reveal a functionally distinct early neural stem cell stage. *Genes Dev* 2008; **22**: 152–165. [Medline] [CrossRef]
28. **Watters AK, Rom S, Hill JD, Dematatis MK, Zhou Y, Merkel SF, Andrews AM, Cena J, Potula R, Skuba A, Son YJ, Persidsky Y, Ramirez SH.** Identification and dynamic regulation of tight junction protein expression in human neural stem cells. *Stem Cells Dev* 2015; **24**: 1377–1389. [Medline] [CrossRef]
29. **Ikenouchi J, Matsuda M, Furuse M, Tsukita S.** Regulation of tight junctions during the epithelium-mesenchyme transition: direct repression of the gene expression of claudins/occludin by Snail. *J Cell Sci* 2003; **116**: 1959–1967. [Medline] [CrossRef]
30. **Cano A, Pérez-Moreno MA, Rodrigo I, Locascio A, Blanco MJ, del Barrio MG, Portillo F, Nieto MA.** The transcription factor snail controls epithelial-mesenchymal transitions by repressing E-cadherin expression. *Nat Cell Biol* 2000; **2**: 76–83. [Medline] [CrossRef]
31. **Yoshida S, Kato T, Kanno N, Nishimura N, Nishihara H, Horiguchi K, Kato Y.** Cell type-specific localization of Ephs pairing with ephrin-B2 in the rat postnatal pituitary gland. *Cell Tissue Res* 2017; **370**: 99–112. [Medline] [CrossRef]
32. **Kosodo Y, Röper K, Haubensak W, Marzesco AM, Corbeil D, Huttner WB.** Asymmetric distribution of the apical plasma membrane during neurogenic divisions of mammalian neuroepithelial cells. *EMBO J* 2004; **23**: 2314–2324. [Medline] [CrossRef]